PHYSICS AND CHEMISTRY OF SOLID STATE
V. 27, No. 2 (2026) pp. 299-309
Section: Physics

DOI: 10.15330/pcss.27.2.299-309

Vasyl Stefanyk Carpathian National University

ФІЗИКА І ХІМІЯ ТВЕРДОГО ТІЛА
Т. 27, № 2 (2026) С. 299-309
Фізико-математичні науки

UDC: 539.2

ISSN 1729-4428 (Print)
ISSN 2309-8589 (Online)

T.S. Kavetskyy[1,2,3], O.I. Matskiv[1], O. Šauša[2,4], H. Švajdlenková[4,5], V.M. Soloviev[3,7], A.O. Bielinskyi[6,7], A.V. Tuzhykov[3], J. Ostrauskaite[8], A.E. Kiv[3,9]

A correlation between formation of free radicals and double bonds conversion during photopolymerization by EPR and NIR study and complex systems theory approach

[1]*Drohobych Ivan Franko State Pedagogical University, Drohobych, Ukraine, kavetskyy@yahoo.com, omackiv@gmail.com;*
[2]*Institute of Physics, Slovak Academy of Sciences, Bratislava, Slovakia;*
[3]*South Ukrainian National Pedagogical University named after K.D. Ushynsky, Odesa, Ukraine, kiv.arnold20@gmail.com, vnsoloviev2016@gmail.com;*
[4]*Department of Nuclear Chemistry, FNS, Comenius University, Bratislava, Slovakia, ondrej.sausa@savba.sk, helena.svajdlenkova@savba.sk;*
[5]*Polymer Institute, Slovak Academy of Sciences, Bratislava, Slovakia;*
[6]*State University of Economics and Technology, Kryvyi Rih, Ukraine;*
[7]*Kyiv National Economic University named after Vadym Hetman, Kyiv, Ukraine;*
[8]*Kaunas University of Technology, Kaunas, Lithuania;*
[9]*Ben-Gurion University of the Negev, 84105 Beer-Sheva, Israel*

The in-situ photopolymerization of acrylated epoxidized soybean oil (AESO) and vanillin dimethacrylate (VDM) with a photoinitiator (2,2-dimethoxy-2-phenylacetophenone) (DMPA) is studied by using electron paramagnetic resonance (EPR) and near-infrared (NIR) spectroscopy methods. A correlation between a concentration of free radicals deduced from EPR spectra and double bond conversion peak area deduced from NIR spectra as a function of UV-irradiation time for the investigated polymer composite is detected. The observed correlation is agreed well with the prediction of photopolymerization and photodegradation phenomena within a complex systems theory approach.

Keywords: photopolymerization, photodegradation, UV light, irradiation, polymers, composite, EPR spectroscopy, IR spectroscopy, structure, properties, complex systems theory.

Received 06 October 2025; Accepted 12 June 2026; Published 22 June 2026.

Introduction

The process of photopolymerization of acrylated epoxidized soybean oil (AESO) and vanillin dimethacrylate (VDM) with and without a photoinitiator (PI) (2,2-dimethoxy-2-phenylacetophenone) (DMPA) has been recently studied by positron annihilation lifetime spectroscopy (PALS), infrared (IR) and electron paramagnetic resonance (EPR) spectroscopy [1-4]. The effect of aromatic rings in AESO-VDM series on the local free volume and diffusion properties of polymer matrix [1, 2] and photopolymerization and photodegradation processes [3, 4] in the cured polymers after long-term UV light exposure have been reported.

In this work, a kinetics of photopolymerization of AESO:VDM (1:0.5) with PI is studied by using EPR and NIR spectroscopy during UV-irradiation. The obtained results showed a correlation between a concentration of free radicals deduced from EPR spectra and double bond conversion peak area deduced from NIR spectra as a function of irradiation time for the investigated polymer composite. A complex systems theory approach was used to clarify the observed phenomena.

I. Experimental

The in-situ photopolymerization of the AESO:VDM (1:0.5) with PI sample was done with UV lamp (365 nm). The flux density at the sample surface was 22 mW/cm^2. The EPR measurements were carried out on the Varian E4 spectrometer, X-band at constant frequency ~9.47 GHz. For the NIR experiment, the sample was measured in a fiber-coupled cuvette holder BW Tek with two optical fiber cables of diameter 100 μm connected to BW Tek detector (Sol. 2.2) and light source BPS 2.0 with the spectral range (350-2600 nm). The NIR spectra were registered in the wavenumber range 4500-9200 cm^{-1}. The intensity of the absorption band at 6172 cm^{-1} reflects the degree of double bond conversion (DBC), i.e., consumption of monomers (AESO, VDM), during the photopolymerization; and thus, the area of this band was taken as a controlled parameter deduced from the NIR spectra.

II. Results and Discussion

2.1. EPR and NIR data.

The time constant of radical decay (often denoted as τ) expresses how quickly the concentration of radicals in a system decreases due to their decay (termination or recombination). If we consider the simple case of bimolecular radical termination: R· + R· → product R, the rate of radical decay is: $-d[R\cdot]/dt = k_t[R\cdot]^2$, where [R·] is the concentration of radicals, k_t is the termination rate constant.

The time constant is defined as the characteristic time for the radical concentration to decrease. For this second order reaction, it can be approximated as: $\tau \approx 1/(k_t\,[R\cdot]_0)$, where $[R\cdot]_0$ is the starting concentration of radicals, k_t is the termination rate constant. Let's denote k, expressed in the value per second, as a radical decay rate constant (i.e., the pseudo-first-order rate constant for radical decay).

The dependence of the concentration of free radicals and the radical decay rate constant (k) according to EPR data for the studied polymer AESO:VDM (1:0.5) with the photoinitiator (PI) during the photopolymerization process as a function of UV-irradiation time is presented in Figure 1. The concentration of free radicals was estimated according to the recorded EPR spectra as a peak area and the rate constant k was calculated by extrapolating this peak area as a function of time. A typical representative of the EPR spectrum measured is shown in Figure 2.

The dependence of the concentration of free radicals according to EPR data and the peak area of DBC (doble bonds conversion) of double bonds C=C according to NIR data for the AESO:VDM (1:0.5) with the photoinitiator (PI) during the photopolymerization process as a function of UV-irradiation time is presented in Figure 3. A typical representative of the NIR spectrum measured is shown in Figure 4.

A correlation between a concentration of free radicals and double bond conversion (DBC) peak area as a function of UV-irradiation time for the investigated polymer composite is detected. In particular, after zero time when reaction is started, there is a minimum concentration of free radicals and maximum of DBC peak area. With increasing of UV-irradiation time, the concentration of free radicals increases and DBC peak area decreases. A feature nearby 55 s (a maximum concentration of free radicals and a plateau of minimum of DBC peak area) could be due to the efficient decay (termination or recombination) of free radicals as shown by the rapid decreases of the radical decay rate constant (k) in Figure 1.

In the previous study [3,4], the EPR results showed that irradiation leads to maximum radical generation due to photoinitiator activation, whereas in the absence of light, the radicals gradually decay through polymerization and termination reactions, resulting in a decreased radical concentration. This finding is now supported by the observed correlation between formation of free radicals and double bonds conversion during photopolymerization.

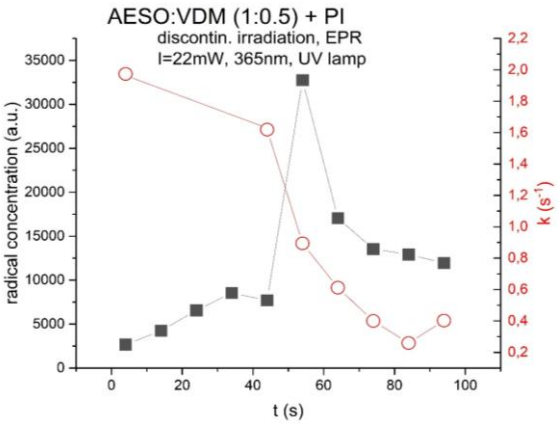

Fig. 1. The dependence of the concentration of free radicals (closed squares) and the radical decay rate constant (k) (open circles) according to EPR data for the AESO:VDM (1:0.5) with the photoinitiator (PI) during the photopolymerization process as a function of UV-irradiation time.

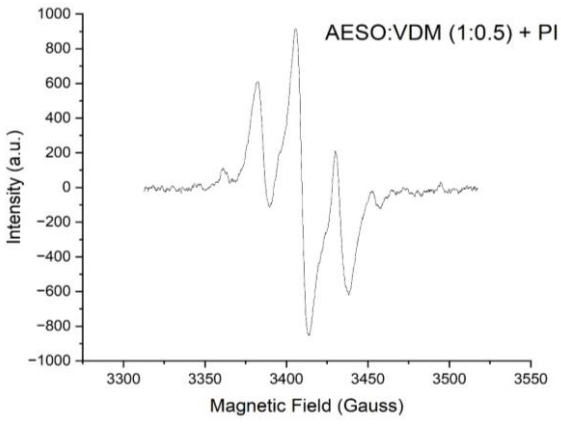

Fig. 2. The representative EPR spectrum for the AESO:VDM (1:0.5) with the photoinitiator (PI).

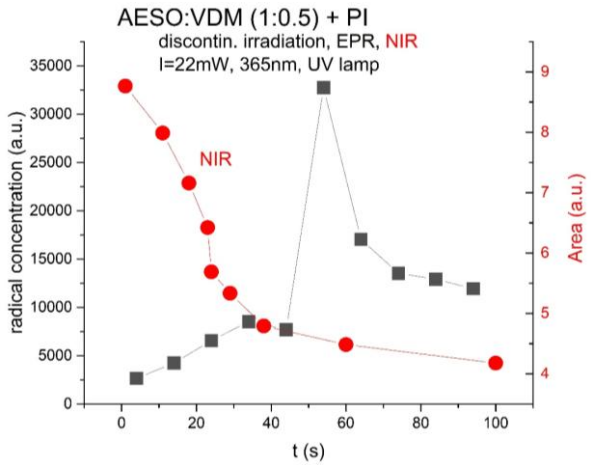

Fig. 3. The dependence of the concentration of free radicals according to EPR data and the peak area of DBC (doble bonds conversion) of double bonds C=C according to NIR data for the AESO:VDM (1:0.5) with the photoinitiator (PI) during the photopolymerization process as a function of UV-irradiation time.

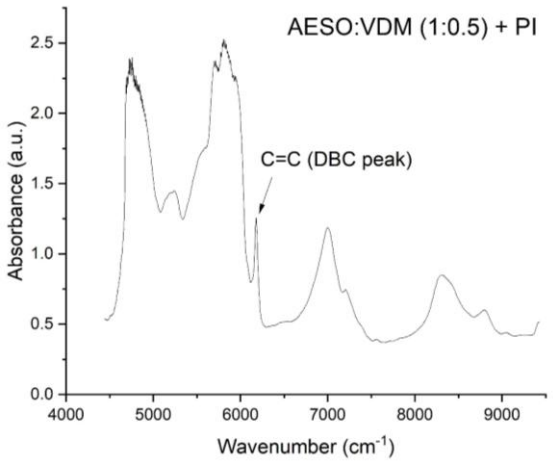

Fig. 4. The representative NIR spectrum for the AESO:VDM (1:0.5) with the photoinitiator (PI).

2.2. Complex systems theory approach.

The conceptualization of physical and chemical systems through the framework of complexity theory constitutes a major conceptual turn in contemporary physical science. Emerging in the mid-twentieth century, this framework was shaped by attempts to explain collective behavior, phase transitions, and the spontaneous emergence of order in systems composed of many interacting elements [5]. A decisive contribution was made by Ilya Prigogine, whose theory of dissipative structures showed that systems maintained far from thermodynamic equilibrium may undergo self-organization rather than simple relaxation, thereby extending the scope of classical thermodynamics [5-8]. In parallel, Hermann Haken developed synergetics as a mathematical language for describing coherent macroscopic behavior arising from nonlinear interactions among many components [9]. These ideas were later reinforced by stochastic thermodynamics, which recast irreversibility in terms of trajectory-level fluctuations and their relation to entropy production [10-12]. Within this framework, the Jarzynski equality connects nonequilibrium work fluctuations with equilibrium free-energy differences, whereas the Crooks fluctuation theorem makes the time-directionality of driven processes explicit by relating the probability of a trajectory to that of its time-reversed counterpart under the reverse protocol [10, 11]. Taken together, these results provide a rigorous basis for interpreting temporal asymmetry in observed dynamics as a quantitative manifestation of dissipation and nonequilibrium behavior.

The mathematical frameworks of non-linear dynamics, chaos theory, and fractal statistics further expanded the capacity to quantitatively analyze complex systems whose locally deterministic dynamics can nevertheless generate irregular, unpredictable, and emergent macroscopic behavior [13, 14]. As emphasized in the National Academy of Sciences colloquium on self-organized complexity, such systems commonly exhibit fractal statistics, scale invariance, and power-law distributions [15]. These properties are often quantified through scaling measures such as the generalized Hurst exponent and fractal dimension, the latter being a central construct in Mandelbrot's formulation of fractal geometry [16, 17]. Rather than remaining at a purely phenomenological level, complexity theory seeks to explain how relatively simple microscopic interaction rules give rise to self-organizing macroscopic structures across multiple spatial and temporal scales [14, 18].

In contemporary materials science and chemical physics, the application of complexity theory to self-organized phenomena is particularly relevant to the study of photopolymerization. Photopolymerization is a light-driven curing process in which irradiation generates reactive species that rapidly convert liquid monomer – oligomer formulations into highly cross-linked polymer networks. Because this transformation is sustained by continuous external energy input and proceeds through coupled reaction, diffusion, thermal, and optical feedbacks, it can be understood as a nonequilibrium dissipative process. Under UV irradiation, the system passes through a rapid sequence of nonlinear physicochemical changes, including radical generation, heat release, viscosity growth, diffusion limitation, and gelation, which collectively govern the emergence of the final polymer network structure [18-21]. The dynamics of this network formation, as well as the subsequent structural evolution and photodegradation of the polymers under prolonged UV exposure, represent critical areas of study for understanding the complete lifecycle of these complex driven systems [4].

The transition from a disordered liquid formulation to a cross-linked solid network is accompanied by a pronounced reduction in configurational freedom and local free volume, together with the emergence of an increasingly constrained and topologically heterogeneous structure [22, 23]. This network-forming process is governed by a tightly coupled interplay among reaction kinetics, diffusion-controlled termination, oxygen

inhibition, and localized exothermic heat generation [21, 24]. As free-radical photopolymerization advances, rising viscosity and restricted chain mobility promote autoacceleration, commonly known as the Trommsdorff-Norrish effect, because bimolecular termination becomes increasingly suppressed while propagation remains operative [18, 25]. The resulting spatiotemporal temperature heterogeneities and dissipation patterns may therefore be interpreted as macroscopic manifestations of the underlying microscopic network self-organization [20, 21].

The concept of self-organized criticality, introduced by Bak, Tang, and Wiesenfeld, states that certain driven dissipative systems can evolve toward critical regimes characterized by avalanche-like relaxation, scale invariance, and power-law statistics [26, 27]. Photopolymerization is not a self-organized critical system in the strict sense, since it is a transient and continuously driven curing process; nevertheless, the stages of gelation and vitrification exhibit analogous features of critical-like restructuring, manifested in abrupt changes in network connectivity, mobility, and relaxation behavior during cure [18, 20]. In polymerizing networks, these transformations are accompanied by anomalous dielectric relaxation and pronounced multiscale thermo-kinetic fluctuations, which have been documented both in curing studies and in recent multifractal analyses of photopolymerization signals [28, 29]. Accordingly, time-series irreversibility provides a suitable quantitative framework for probing self-organization in such dissipative chemical systems, because temporal asymmetry can be inferred directly from experimental trajectories by data-driven methods based on visibility graphs or ordinal patterns, without requiring a fully specified mechanistic model [30, 31].

Several complementary classes of estimators have been developed to detect and quantify irreversibility in empirical time series. Symbolic approaches compare the statistics of short ordinal patterns with those of their time-reversed counterparts; in this context, the permutation-pattern framework introduced by Bandt and Pompe provides a simple and computationally efficient representation that is robust to monotonic amplitude transformations and does not require arbitrary amplitude binning [32]. Building on this idea, Zanin *et al.* proposed an irreversibility measure based on pairing each permutation pattern with its reversed analogue and quantifying the discrepancy between the corresponding ordinal distributions by means of the Kullback-Leibler divergence, showing that this construction is temporally local, statistically testable, and rapidly convergent in practice [33]. In parallel, visibility-graph approaches transform a time series into a network in which vertices correspond to observations and edges encode mutual visibility relations between them [34, 35]. Within this framework, Lacasa *et al.* showed that the Kullback-Leibler divergence between the in-degree and out-degree distributions of a directed horizontal visibility graph provides a consistent estimator of time irreversibility for stationary processes, and that, in nonequilibrium steady states, it constitutes a lower bound on entropy production [30]. Lacasa and Flanagan subsequently extended the formalism to non-stationary signals, demonstrating that visibility-graph-based irreversibility measures can remain finite and informative even in settings where conventional reversibility tests become problematic [36]. Donges, Donner, and Kurths further complemented the degree-based approach by introducing tests based on retarded and advanced local clustering coefficients, thereby probing short-range topological asymmetries and revealing nonlinear temporal structure beyond simple drift or trend effects [37].

These approaches have already been applied across a wide range of empirical domains, including sleep electroencephalography [38], heart-rate variability [39], climate variability and sea-surface-temperature dynamics [40], financial time series [41], and electromagnetic turbulence in non-thermal plasmas [42], with a recent review summarizing the broader methodological landscape [43]. Furthermore, the translation of complex network methods into materials science has proven highly effective for characterizing structural and dynamic transformations, such as the plastic deformation dynamics in metals [44]. More recently, these network-based analytical frameworks have been successfully combined with spectroscopic and positron annihilation techniques to probe the complex microstructural evolution during photopolymerization [3]. To the best of our knowledge, however, such irreversibility estimators have not yet been used to monitor an in-situ chemical self-organization event such as UV photopolymerization. This context is especially demanding because the process spans, within a single thermal record, quasi-equilibrium fluctuations before irradiation, a strongly nonequilibrium exothermic autoacceleration stage, and a slow relaxation regime after gelation and vitrification. Since the three estimators employed here capture different structural facets of temporal asymmetry – global amplitude asymmetry, local topological asymmetry, and amplitude-invariant ordinal asymmetry – their combined use can disclose complementary stages of the reaction, including the onset of nonequilibrium dynamics, the peak of autoacceleration, the crossover to diffusion-controlled behavior, and the approach to a new quasi-stationary state.

The present work fills this gap. We record the *in-situ* temperature trajectory during UV photopolymerization of AESO:VDM (1:0.5) with PI formulation and analyze it with a sliding-window combination of the three irreversibility estimators. Our central contribution is to show that time irreversibility is a robust, multiscale hallmark of photopolymerization self-organization, that each of the three measures carries a distinct and physically interpretable signature of the underlying radical-chain/diffusion kinetics, and that their combination provides a compact, model-free description of the transition from the liquid monomer mixture, through the Trommsdorff exotherm, to the vitrified crosslinked network.

2.3. Visibility graph analysis and network topological asymmetry.

The visibility graph algorithm, originally proposed by Lacasa *et al.* [34] and heavily expanded for the assessment of non-stationary processes by Lacasa and Flanagan [36], provides a deterministic, parameter-free geometric transformation of a univariate time series into a complex

network. This transformation successfully preserves the inherent dynamical properties, fractal characteristics, and non-linearities of the original signal within the topological architecture (nodes and edges) of the resulting graph.

Given a recorded time series of highly resolved temperature fluctuations, denoted mathematically as an ordered set of real-valued data points $X = \{x_1, x_2, \dots, x_N\}$ observed at strictly ordered discrete times $t_1, t_2, \dots, t_N$, the NVG constructs an undirected graph comprised of exactly N nodes. Each specific node $i \in [1, N]$ represents a specific temporal observation x_i. The fundamental connectivity rule dictates that two nodes i and j (assuming chronological order where $t_i < t_j$) are connected by an edge if and only if a straight "line of sight" can be drawn between their corresponding data points on a standard Cartesian plot without intersecting any intermediate data point. Mathematically, this convexity criterion establishes that for any intermediate node k existing between i and j ($t_i < t_k < t_j$), the amplitude value x_k must strictly satisfy the following geometric inequality:

$$x_k < x_i + \frac{t_k - t_i}{t_j - t_i}\left(x_j - x_i\right). \quad (1)$$

Because the unidirectional flow of time intrinsically establishes an ordered sequence of events, the seemingly undirected edges of the resulting visibility graph can be mathematically parsed into directed edges. An edge connecting node i to node j ($i < j$) is logically classified as an "advanced" (or outgoing) link from the specific perspective of node i, pointing forward toward the future states of the system. Conversely, this exact same edge is classified as a "retarded" (or incoming) link from the perspective of node j, pointing backward toward the past historical states. This elegant directed formulation permits the explicit decomposition of standard, well-understood complex network properties into past-directed and future-directed components, facilitating a highly sensitive evaluation of time-reversal symmetry.

Network degree asymmetry: The degree of a single node in a network, denoted as k_i, represents the total number of visibility connections it possesses to other nodes. Under the time-directed framework proposed by Donges *et al.* [37], the total degree is explicitly partitioned into the retarded degree k_i^r (the total number of connections to past observations where $j < i$) and the advanced degree k_i^a (the total number of connections to future observations where $j > i$), such that the fundamental relation $k_i = k_i^r + k_i^a$ holds true. By computing the empirical probability distributions of the retarded and advanced degrees across a designated temporal window – denoted functionally as $P(k^r)$ and $P(k^a)$, respectively – the physical reversibility of the system's thermal dynamics can be statistically assessed.

Local clustering coefficient asymmetry: To capture deeper, higher-order topological correlations and local geometric rigidity, the local clustering coefficient C_i is similarly decomposed. In graph theory, the standard clustering coefficient measures the probability that two randomly selected neighbors of node i are themselves directly connected (forming a visible triangle). The time-directed retarded local clustering coefficient C_i^r evaluates this connectivity density exclusively among the past neighbors of node i, determining how tightly clustered the system's history was. The advanced local clustering coefficient C_i^a evaluates the connectivity exclusively among future neighbors, assessing the density of upcoming thermodynamic states. The corresponding empirical probability distributions are denoted as $P(C^r)$ and $P(C^a)$.

To establish a singular, quantitative index of time series irreversibility based on these extracted network topologies, the KL divergence – a foundational metric of relative entropy – is computed to precisely determine the statistical distance between the advanced and retarded probability distributions. The KL divergence for the degree distribution, denoted in this study as $\mathrm{Dist}_{\mathrm{deg}}$, is calculated using the standard formulation:

$$D_{KL}[P(k^r) \parallel P(k^a)] = \mathrm{Dist}_{\mathrm{deg}} = \sum P(k^r) \ln\left[\frac{P(k^r)}{P(k^a)}\right]. \quad (2)$$

Similarly, the specific KL divergence for the clustering coefficient, denoted as $\mathrm{Dist}_{\mathrm{clust}}$, is computed iteratively between $P(C^a)$ and $P(C^r)$. If the underlying physico-chemical process is perfectly reversible and resting at equilibrium, the future and past network topologies will be statistically indistinguishable, and the probability distributions will map onto each other perfectly, yielding a theoretical KL divergence approaching exactly zero. Any positive deviation from zero strictly signifies the mathematical presence of time irreversibility, acting as a highly robust, non-linear indicator of non-equilibrium dynamics, entropy production, and deterministic phase transitions occurring within the curing polymerizing medium.

2.4. Permutation patterns and ordinal probability divergence.

As a highly complementary measure of system complexity, the symbolic dynamic approach based on permutation patterns provides an exceptionally noise-robust and computationally efficient method for quantifying time series irreversibility at the micro-structural scale. Originally conceptualized by Bandt and Pompe for measuring time series complexity [32], and subsequently adapted specifically for irreversibility testing by Zanin *et al.* [33], this method evaluates the asymmetric prevalence of specific ordinal microstates occurring in standard chronological order versus their exact time-reversed geometric counterparts.

The application of the permutation pattern algorithm requires the strict initial definition of an embedding dimension, denoted as d_E, which dictates the length of the ordinal sequences to be continuously extracted from the original time series. The raw time series of temperature fluctuations X is systematically partitioned into heavily overlapping vectors of length d_E. For each individual vector, the actual physical data points are sorted in ascending amplitude order, and the specific sequence of their original temporal indices is recorded as the "permutation pattern" (often referred to as the ordinal symbol). Because there are exactly $d_E!$ mathematically possible ways to uniquely order d_E distinct values, the infinite continuous state space of the time series is

effectively discretized into a highly manageable, finite state space consisting of exactly $d_E!$ unique symbolic microstates.

The profound essence of the irreversibility test proposed by Zanin *et al.* [33] lies in the deliberate pairing of time-reversed patterns. Every single permutation pattern generated by the sequence has one, and only one, specific time-reversed counterpart. For a chosen embedding dimension of $d_E = 3$, which generates $3! = 6$ possible distinct patterns, the sequences can be logically paired according to their strict temporal symmetry. For example, a monotonically increasing thermal pattern represented by the ordinal sequence $(0, 1, 2)$ physically represents a strict, uninterrupted temperature rise over three consecutive measurements. Its exact time reversal is the monotonically decreasing pattern $(2, 1, 0)$, representing sequential cooling. The other discrete mathematical pairings include $(1, 0, 2) \leftrightarrow (2, 0, 1)$ and $(1, 2, 0) \leftrightarrow (0, 2, 1)$.

A completely reversible, stationary thermodynamic process mandates that the empirical probability of observing any specific permutation pattern must perfectly equal the probability of observing its exact time-reversed counterpart over a sufficiently large sampling window. If, for instance, $P(0, 1, 2) \neq P(2, 1, 0)$, it proves that the statistical properties of the system are heavily dependent on the specific direction of time flow, confirming that the physical signal is definitively irreversible and generating entropy.

To mathematically aggregate this localized ordinal asymmetry into a single, comprehensive statistical metric for the evaluated time series window, the KL divergence is once again employed. The specific divergence is computed between the total probability distribution of all forward permutation patterns, denoted P_f, and the overall probability distribution of their corresponding time-reversed patterns, denoted P_r:

$$D_{KL}\left[P_f \parallel P_r\right] = \sum_{i=1}^{d_E!} P_f(i) \ln\left[\frac{P_f(i)}{P_r(i)}\right]. \quad (3)$$

In the specific context of the AESO:VDM photopolymerization reaction, calculating the KL divergence of these permutation patterns provides an ultra-sensitive gauge of local thermodynamic directionality. A sharp, well-defined rise in this permutation metric unambiguously indicates that certain micro-scale energetic trajectories – such as ultra-fast, sharp temperature spikes driven by radical propagation followed by heavily constrained, slow cooling curves – are completely dominating the temporal landscape. This ordinal dominance is a direct, unavoidable consequence of the highly exothermic nature of the non-linear cross-linking cascade occurring far from equilibrium.

To synthesize the diverse analytical frameworks employed in this study, Table 1 provides a comprehensive overview of the three complexity estimators, their corresponding extracted mathematical properties, and their specific diagnostic roles in tracking the structural evolution of the polymerizing matrix.

2.5. Sliding-window framework for resolving transient dynamics.

Both the advanced visibility graph methodology and the permutation pattern framework derive their powerful statistical metrics from a defined, static set of data points. However, the AESO:VDM photopolymerization process is an explicitly, violently transient phenomenon; the structural architecture, local free volume, and thermodynamic properties of the matrix are evolving constantly from the exact millisecond the UV lamp is engaged until terminal vitrification. To accurately and continuously track the system's rapid transition between different thermodynamic states, the various irreversibility measures must be computed dynamically rather than globally.

This dynamic resolution is meticulously achieved via a systematic, algorithmically defined sliding-window approach. A finite fragment of the localized temperature fluctuation time series is completely isolated within a predefined temporal window (e.g., of a designated length $w = 500$ seconds). Within the strict confines of this specific window, the complete suite of complexity measures – the advanced and retarded degree distributions, the advanced and retarded local clustering coefficient distributions, and the forward and reversed permutation pattern distributions – are rigorously calculated. Once the three distinct KL divergence metrics

Table 1.

Summary of the computational complexity methods, their extracted mathematical properties, and their specific diagnostic purposes in the analysis of the photopolymerization process.

Analytical Method	Extracted Mathematical Property	Specific Purpose in the Photopolymerization Study
Natural Visibility Graph (NVG)	Network Degree Asymmetry ($\mathrm{Dist}_{\mathrm{deg}}$)	Identifies large-scale connectivity shifts, macroscopic symmetry breaking, and macro-structural quasi-phase transitions.
NVG Clustering	Clustering Asymmetry ($\mathrm{Dist}_{\mathrm{clust}}$)	Assesses localized topological rigidities, immediate physical defect formation, and the restriction of local degrees of freedom.
Permutation Patterns	Ordinal Probability Divergence ($\mathrm{Dist}_{\mathrm{perm}}$)	Captures micro-level thermodynamic flow, localized thermal irreversibility, and the strict directionality of entropy production.
Sliding-Window D_{KL} Framework	Continuous Iterative Relative Entropy	Continuously tracks the progression of self-organization and physical state changes across all reaction stages in real-time.

($\mathrm{Dist_{deg}}$, $\mathrm{Dist_{clust}}$, $\mathrm{Dist_{perm}}$) are extracted for this initial window, the boundary of the window is shifted forward in time by a highly specific, predetermined step size (e.g., $\Delta t = 1$ second). The mentioned parameters have been used to get the presented in this study results.

This precise computational procedure is repeated iteratively and continuously until the entirety of the experimental time series is completely exhausted. The resulting mathematical output is a novel set of secondary time series that directly describe the chronological evolution of the system's macroscopic irreversibility over the course of the reaction. By directly correlating the dynamic trends of these extracted complexity measures against the raw profile of the original temperature data, the precise temporal moments of self-organization, structural constraint, and distinct quasi-phase transitions within the AESO:VDM matrix can be isolated, quantified, and mechanistically interpreted with unparalleled accuracy.

2.6. Network geometry and macroscopic structural reorganization.

The comparative dynamics mapping the raw temperature fluctuations against the visibility-graph-derived irreversibility measures – specifically the KL-divergence of the network degree ($\mathrm{Dist_{deg}}$) and the local clustering coefficient ($\mathrm{Dist_{clust}}$) presented in Figure 5 – provide a breathtaking topological translation of this complex physical process.

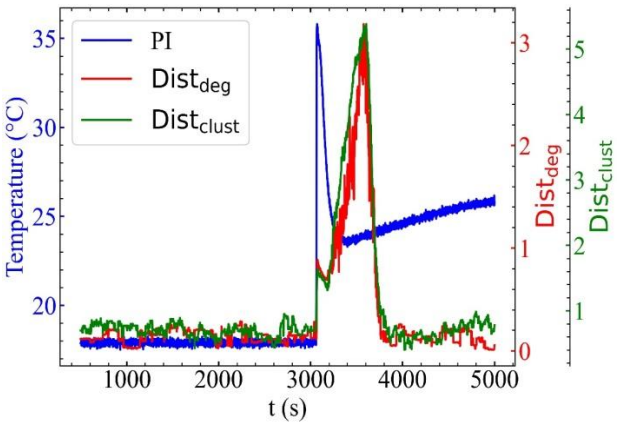

Fig. 5. Comparative dynamics mapping the raw in-situ temperature fluctuations against the visibility-graph-derived irreversibility measures, specifically the Kullback-Leibler divergence of the network degree ($\mathrm{Dist_{deg}}$) and the local clustering coefficient ($\mathrm{Dist_{clust}}$) for the AESO:VDM (1:0.5) with the photoinitiator (PI).

Prior to irradiation (t < 3100 s), the graph topology derived from the baseline thermal noise remains largely symmetric: the probability of future-directed (advanced) links closely matches that of past-directed (retarded) links, yielding $\mathrm{Dist_{deg}}$ values clustered near 0.1 and $\mathrm{Dist_{clust}}$ values around 0.8. Within the visibility-graph framework, such weak asymmetry is consistent with a near-reversible baseline regime in which no pronounced temporal directionality is expressed in the thermal microfluctuations.

Once the UV lamp is switched on, both $\mathrm{Dist_{deg}}$ and $\mathrm{Dist_{clust}}$ exhibit pronounced and highly structured increases. Although the temperature responds almost immediately at $t \approx 3100$ s, the strongest peaks of the irreversibility measures are shifted to the subsequent interval $t \approx$ 3200-3800 s, that is, to the stage of cooling and structural relaxation. This delay is consistent with the known sequence of free-radical photopolymerization, in which light-induced initiation is followed by rapid network formation, diffusion-controlled relaxation, gelation/vitrification, and autoacceleration of the Trommsdorff-Norrish type [18, 20, 28]. This interpretation is also chemically plausible for AESO:VDM systems, because AESO contributes flexible aliphatic segments, whereas VDM introduces rigid aromatic methacrylate units; increasing the VDM fraction has been shown to reduce local free volume and alter network packing in the cured matrix [2, 45, 46].

In Figure 3, the surge in $\mathrm{Dist_{deg}}$ – reaching an extreme peak at $t \approx 3600$ s – indicates that the broad hierarchical structure of the temperature profile has become highly skewed and temporally biased. The rapid heating phase followed by a slower, structurally constrained dissipation phase guarantees that the high-temperature graph nodes created shortly after initiation "see" very far into the future (possessing exceptionally high advanced degree) but look back onto a drastically different, flat past. This massive network asymmetry reflects the macroscopic self-organization of the sample: the fluid convective dynamics that completely governed heat transfer in the liquid past are irrevocably replaced by conductive heat transfer moving laboriously through a solidifying, rigid polymer lattice.

Concurrently, in Figure 5, the sharp, monumental rise in $\mathrm{Dist_{clust}}$ – peaking at $t \approx 3600$ s – highlights an intense, unavoidable localization of irreversible physical events. The local clustering coefficient evaluates the connectivity of immediate, localized topological neighborhoods. In the strict physical context of the AESO:VDM matrix, this localized mathematical asymmetry corresponds directly to the localized formation and kinetic trapping of orientational defects. Because the polymerization proceeds at an exceptional velocity under the high flux density of 22 mW/cm^2, the growing polymer chains and the bulky, sterically hindering aromatic VDM rings become violently trapped before they can physically relax into their optimal, low-energy spatial configurations. These permanently trapped orientational defects drastically alter the local dielectric and thermodynamic relaxation behavior of the material, which translates directly into highly localized, strictly direction-dependent thermal fluctuations. The $\mathrm{Dist_{clust}}$ metric essentially quantifies the rapid topological "locking" of the polymer matrix as free volume diminishes catastrophically, and steric hindrance from the VDM rings forces the transition toward a highly stressed glassy state. By $t \approx 3900$ s, as the matrix vitrifies completely and the thermal profile enters its slow, linear, diffusion-controlled rise, both network metrics crash back down to baseline, indicating that a new, solid-state equilibrium has been achieved.

2.7. Ordinal asymmetry and microstate thermodynamic irreversibility.

While visibility graphs capture macroscopic geometric shifts in the thermal time series, permutation

patterns explicitly evaluate the prevalence of specific chronological sequences (microstates) versus their exact mathematical time-reversals. The comparative dynamics utilizing the KL-divergence based purely on permutation patterns ($\mathrm{Dist}_{\mathrm{perm}}$), presented in Figure 6, provide the most granular, noise-resistant view of the thermodynamic entropy production occurring within the polymerizing matrix.

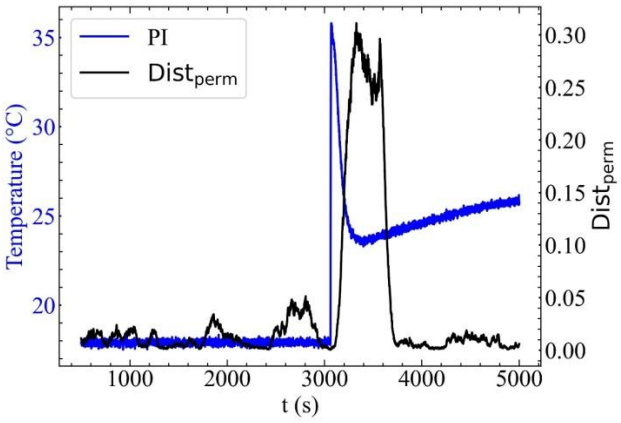

Fig. 6. Comparative dynamics mapping the raw temperature fluctuations against the ordinal probability divergence ($\mathrm{Dist}_{\mathrm{perm}}$) derived from permutation patterns, illustrating the microstate thermodynamic irreversibility and entropy production within the polymerizing matrix for the AESO:VDM (1:0.5) with the photoinitiator (PI).

The application of this ordinal measure to the light-switching-on stage reveals a distinct, massively sustained peak in ordinal irreversibility. Prior to $t \approx 3100$ s, $\mathrm{Dist}_{\mathrm{perm}}$ rests near 0.01, indicating high reversibility of the liquid's thermal noise. Exactly correlating with the massive thermal spike and subsequent exponential cooling curve, $\mathrm{Dist}_{\mathrm{perm}}$ erupts into a broad, jagged peak, maintaining values between 0.20 and 0.30 within $t \approx 3200$-3800 s. During the absolute height of the radical propagation and subsequent autoacceleration, the local temporal profiles of energy generation and dissipation become strictly, undeniably unidirectional.

An ordinal permutation pattern such as $(0, 1, 2)$ – physically representing sequential localized heating as a new covalent bond forms and violently releases enthalpy – will occur with exponentially higher frequency than its exact time-reversed cooling counterpart $(2, 1, 0)$ over the chosen short embedding dimension. This profound ordinal divergence is a direct, undeniable signature of microscopic self-organization. Because the chemical system is continuously driven far from thermal equilibrium by the continuous 365 nm photon flux, it continuously produces systemic entropy. The permutation pattern analysis definitively demonstrates that the structural evolution of the AESO:VDM copolymer is absolutely not a smooth, continuous thermodynamic transition, but rather a violent sequence of highly deterministic, irreversible micro-events that force the system along a singular arrow of time.

Furthermore, as the interpenetrating polymer network reaches the critical gel point and rapidly approaches total vitrification, the reaction kinetics fundamentally shift from being chemically controlled to diffusion-controlled. The highly rigid nature of the AESO-VDM cross-links dictates that unreacted monomers, photoinitiator fragments, and live macroradicals become physically immobilized within the narrowing lattice. The permutation irreversibility measure correlates tightly and perfectly with this physical immobility; as the system rapidly loses its internal degrees of freedom, the available pathways for thermal dissipation become highly restricted and specific, drastically exacerbating the mathematical disparity between forward and reverse ordinal patterns.

2.8. Summary remarks

The rigorous application of these sophisticated complexity measures to the AESO:VDM photopolymerization process yields profound insights that extend far beyond the realm of theoretical thermodynamics. The proven ability to precisely quantify both the exact moment and the physical magnitude of structural quasi-phase transitions – using purely non-invasive, continuous temperature fluctuation data – presents a highly transformative analytical paradigm for optimizing biobased polymer manufacturing and resin formulation.

By systematically utilizing the sliding-window irreversibility metrics ($\mathrm{Dist}_{\mathrm{deg}}$, $\mathrm{Dist}_{\mathrm{clust}}$, and $\mathrm{Dist}_{\mathrm{perm}}$) as an active feedback mechanism, materials researchers and chemical engineers could theoretically calibrate the UV flux density, the initial AESO:VDM stoichiometric molar ratio, and the exact photoinitiator concentration to achieve a more controlled, gradual evolution of network complexity [47-49]. Rather than forcing the bio-resin system into an instantaneous, violent quasi-phase transition laden with permanent kinetic traps, the manufacturing parameters can be precisely tuned to minimize the extreme peaks of the KL-divergence profiles. A lower, broader, and smoother divergence curve would definitively signify a more reversible, equilibrium-adjacent curing process. This controlled trajectory would allow the growing polymer chains adequate time to undergo vital structural relaxation, optimizing their free-volume distribution and minimizing internal stress before terminal vitrification is achieved.

The exhaustive evaluation of the in-situ photopolymerization of the AESO:VDM system through the rigorous framework of complexity theory brilliantly elucidates the profound relationship between macroscopic observables and microscopic self-organization. By interpreting localized temperature fluctuations not merely as random thermal noise, but as a rich, deeply informative thermodynamic state-space, the analysis successfully isolates the intricate signatures of non-equilibrium dynamics. Ultimately, the synthesis of non-linear network methods, symbolic dynamics, and physical chemistry offers a robust, non-invasive methodology for tracking the exact temporal progression of polymer vitrification, paving the way toward advanced additive manufacturing techniques that leverage the complex self-organizing kinetics of macromolecular assembly.

Conclusion

A kinetics of photopolymerization of the AESO:VDM

(1:0.5) with the photoinitiator (PI) DMPA was studied by using EPR and NIR spectroscopy during UV-irradiation. The obtained results showed a correlation between the concentration of free radicals deduced from EPR spectra and double bond conversion peak area deduced from NIR spectra as a function of irradiation time. The observed correlation is agreed well with the prediction of photopolymerization and photodegradation phenomena within the complex systems theory approach.

Acknowledgments

This work was supported in part by the Ministry of Education and Science of Ukraine (projects Nos. 0125U001054, 0125U002005 and 0125U002033), National Research Foundation of Ukraine (project No. 2020.02/0100), Slovak Grant Agency VEGA (project No. 2/0131/25), and Slovak Research and Development Agency (project No. APVV-21-0335). T.S.K. also acknowledges the SAIA (Slovak Academic Information Agency) for a scholarship in the IPSAS in the framework of the National Scholarship Programme of the Slovak Republic. This work has also received funding through the MSCA4Ukraine project (grant No. 1128327), which is funded by the European Union.

Data Availability Statement: *The original contributions presented in this study are included in the article. Further inquiries can be directed to the corresponding authors.*

Conflicts of Interest: *The authors declare no conflicts of interest.*

Kavetskyy T.S. – PhD in Physics and Mathematics, Associate Professor;
Matskiv O.I. – PhD student;
Šauša O. – PhD in Physics;
Švajdlenková H. – PhD in Chemistry;
Soloviev V.M. – D.Sc. in Physics and Mathematics, Professor;
Bielinskyi A.O. – PhD student;
Tuzhykov A.V. – PhD student;
Ostrauskaite J. – PhD in Physical Sciences, Chemistry, Professor;
Kiv A.E. – D.Sc. in Physics and Mathematics, Professor.

[1] D.P. Královič, K. Cifraničová, O. Šauša, H. Švajdlenková, T. Kavetskyy, A. Kiv, *The process of photopolymerization of acrylated soybean oil-based epoxides investigated by positron annihilation lifetime spectroscopy*, Chemical Papers, 77, 7257 (2023); https://doi.org/10.1007/s11696-022-02607-0.
[2] D.P. Královič, K. Cifraničová, H. Švajdlenková, D. Tóthová, O. Šauša, P. Kalinay, T. Kavetskyy, J. Ostrauskaite, O. Smutok, M. Gonchar, V. Soloviev, A. Kiv, *Effect of aromatic rings in AESO-VDM biopolymers on the local free volume and diffusion properties of polymer matrix*, Journal of Polymers and the Environment, 32, 2336 (2024); https://doi.org/10.1007/s10924-023-03097-1.
[3] T. Kavetskyy, O. Zubrytska, M. Stievenard, O. Šauša, H. Švajdlenková, V. Soloviev, A. Bielinskyi, J. Ostrauskaite, A. Kiv, *Complex network methods, PALS, ATR-FTIR and EPR study of photopolymerization*, In: P. Petkov, M.E. Achour, C. Popov (Eds.), Nanotechnological Advances in Environmental, Cyber and CBRN Security. NATO Science for Peace and Security Series B: Physics and Biophysics. Springer, Dordrecht, Chap. 19, 265 (2025); https://doi.org/10.1007/978-94-024-2316-7_19.
[4] T.S. Kavetskyy, O.V. Zubrytska, O.I. Matskiv, M. Stievenard, O. Šauša, H. Švajdlenková, V.M. Soloviev, A.O. Bielinskyi, J. Ostrauskaite, A.E. Kiv, *Photopolymerization and photodegradation of polymers after long-term UV light exposure*, Physics and Chemistry of Solid State, 26(4), 718 (2025); https://doi.org/10.15330/pcss.26.4.718-732.
[5] F. Heylighen, *Complexity and Self-organization*, in M.J. Bates & M.N. Maack (Eds.), Encyclopedia of Library and Information Science (3rd ed.), Taylor & Francis, (2009); http://pespmc1.vub.ac.be/PAPERS/ELIS-complexity.pdf.
[6] I. Prigogine, I. Stengers, Order out of Chaos. Bantam Books, (1984).
[7] G. Nicolis, I. Prigogine, *Self-organization in Nonequilibrium Systems: From Dissipative Structures to Order through Fluctuations*, Wiley, (1977).
[8] D. Kondepudi, I. Prigogine, *Modern thermodynamics: From heat engines to dissipative structures (2nd ed.).* Wiley, (2014).
[9] H. Haken, *Information and Self-organization: A Macroscopic Approach to Complex Systems*, Springer-Verlag, (2000).
[10] C. Jarzynski, *Nonequilibrium equality for free energy differences*, Physical Review Letters, 78(14), 2690 (1997); https://doi.org/10.1103/PhysRevLett.78.2690.
[11] G.E. Crooks, *Entropy production fluctuation theorem and the nonequilibrium work relation for free energy differences*, Physical Review E, 60(3), 2721 (1999); https://doi.org/10.1103/PhysRevE.60.2721.
[12] J.M.R. Parrondo, C. Van den Broeck, R. Kawai, *Entropy production and the arrow of time*, New Journal of Physics, 11, 073008 (2009); https://doi.org/10.1088/1367-2630/11/7/073008.
[13] E. Ott, Chaos in Dynamical Systems (2nd ed.), Cambridge University Press, (2002).
[14] M. Mitchell, Complexity: A Guided Tour, Oxford University Press, (2009).
[15] D.L. Turcotte, J.B. Rundle, *Self-organized complexity in the physical, biological, and social sciences*, Proceedings of the National Academy of Sciences, 99 (1), 2463 (2002); https://doi.org/10.1073/pnas.012579399.
[16] B.B. Mandelbrot, The Fractal Geometry of Nature, W.H. Freeman, (1982).

[17] Y. Bar-Yam, *Multiscale variety in complex systems*, Complexity, 9(4), 37 (2004); https://doi.org/10.1002/cplx.20014.
[18] C.N. Bowman, C.J. Kloxin, *Toward an enhanced understanding and implementation of photopolymerization reactions*, AIChE Journal, 54(11), 2775 (2008); https://doi.org/10.1002/aic.11678.
[19] C. Decker, *Kinetic study and new applications of UV radiation curing*, Macromolecular Rapid Communications, 23(18), 1067 (2002); https://doi.org/10.1002/marc.200290014.
[20] M. Lang, S. Hirner, F. Wiesbrock, P. Fuchs, *A review on modeling cure kinetics and mechanisms of photopolymerization*, Polymers, 14(10), 2074 (2022); https://doi.org/10.3390/polym14102074.
[21] A.K. O'Brien, C.N. Bowman, *Modeling thermal and optical effects on photopolymerization systems*, Macromolecules, 36(20), 7777 (2003); https://doi.org/10.1021/ma034070c.
[22] K.S. Anseth, C.M. Wang, C.N. Bowman, *Kinetic evidence of reaction diffusion during the polymerization of multi(meth)acrylate monomers*, Macromolecules, 27(3), 650 (1994); https://doi.org/10.1021/ma00081a004.
[23] H. Švajdlenková, O. Šauša, G. Peer, C. Gorsche, *In situ investigation of the kinetics and microstructure during photopolymerization by positron annihilation technique and NIR-photorheology*, RSC Advances, 8(65), 37085 (2018); https://doi.org/10.1039/C8RA07578F.
[24] C. Decker, A.D. Jenkins, *Kinetic approach of oxygen inhibition in ultraviolet- and laser-induced polymerizations*, Macromolecules, 18(6), 1241 (1985); https://doi.org/10.1021/ma00148a034.
[25] J.S. Young, C.N. Bowman, *Effect of polymerization temperature and cross-linker concentration on reaction diffusion controlled termination*, Macromolecules, 32(19), 6073 (1999); https://doi.org/10.1021/ma9902955.
[26] P. Bak, C. Tang, K. Wiesenfeld, *Self-organized criticality: An explanation of 1/f noise*, Physical Review Letters, 59(4), 381 (1987); https://doi.org/10.1103/PhysRevLett.59.381.
[27] P. Bak, C. Tang, K. Wiesenfeld, *Self-organized criticality*, Physical Review A, 38(1), 364 (1988); https://doi.org/10.1103/PhysRevA.38.364.
[28] S. Montserrat, F. Román, P. Colomer, *Vitrification and dielectric relaxation during the isothermal curing of an epoxy-amine resin*, Polymer, 44(1), 101 (2003); https://doi.org/10.1016/S0032-3861(02)00745-0.
[29] A.E. Kiv, V.N. Soloviev, A.O. Bielinskyi, M.A. Slusarenko, T.S. Kavetskyy, O. Šauša, H. Švajdlenková, I.I. Donchev, N. Hoivanovych, L.I. Pankiv, O.V. Nykolaishyn, O.R. Mushynska, O.V. Zubrytska, A.V. Tuzhykov, M. Kushniyazova, *Multifractal signatures of light-driven self-organization in acrylated epoxidized soybean oil polymers*, Semiconductor Physics, Quantum Electronics & Optoelectronics, 27(3), 366 (2024); https://doi.org/10.15407/spqeo27.03.366.
[30] L. Lacasa, A.M. Núñez, E. Roldán, J.M.R. Parrondo, B. Luque, *Time series irreversibility: A visibility graph approach*, The European Physical Journal B, 85, 217 (2012); https://doi.org/10.1140/epjb/e2012-20809-8.
[31] J.H. Martínez, J.L. Herrera-Diestra, M. Chavez, *Detection of time reversibility in time series by ordinal patterns analysis*, Chaos, 28(12), 123111 (2018); https://doi.org/10.1063/1.5055855.
[32] C. Bandt, B. Pompe, *Permutation entropy: A natural complexity measure for time series*, Physical Review Letters, 88(17), 174102 (2002); https://doi.org/10.1103/PhysRevLett.88.174102.
[33] M. Zanin, A. Rodríguez-González, E. Menasalvas Ruiz, D. Papo, *Assessing time series reversibility through permutation patterns*, Entropy, 20(9), 665 (2018); https://doi.org/10.3390/e20090665.
[34] L. Lacasa, B. Luque, F. Ballesteros, J. Luque, J.C. Nuño, *From time series to complex networks: The visibility graph,* Proceedings of the National Academy of Sciences, 105(13), 4972 (2008); https://doi.org/10.1073/pnas.0709247105.
[35] B. Luque, L. Lacasa, F. Ballesteros, J. Luque, *Horizontal visibility graphs: Exact results for random time series*, Physical Review E, 80(4), 046103 (2009); https://doi.org/10.1103/PhysRevE.80.046103.
[36] L. Lacasa, R. Flanagan, *Time reversibility from visibility graphs of nonstationary processes*, Physical Review E, 92(2), 022817 (2015); https://doi.org/10.1103/PhysRevE.92.022817.
[37] J.F. Donges, R.V. Donner, J. Kurths, *Testing time series irreversibility using complex network methods*, Europhysics Letters, 102, 10004 (2013); https://doi.org/10.1209/0295-5075/102/10004.
[38] H. Xiong, P. Shang, F. Hou, Y. Ma, *Visibility graph analysis of temporal irreversibility in sleep electroencephalograms*, Nonlinear Dynamics, 96(1), 1 (2019); https://doi.org/10.1007/s11071-019-04768-2.
[39] Y. Li, J. Li, J. Liu, Y. Xue, Z. Cao, C. Liu, *Variations of time irreversibility of heart rate variability under normobaric hypoxic exposure*, Frontiers in Physiology, 12, 607356 (2021); https://doi.org/10.3389/fphys.2021.607356.
[40] D. Zhao, X. Yang, W. Song, W. Zhang, D. Huang, *Visibility graph analysis of the sea surface temperature irreversibility during El Niño events,* Nonlinear Dynamics, 111, 17393 (2023); https://doi.org/10.1007/s11071-023-08762-7.
[41] R. Flanagan, L. Lacasa, *Irreversibility of financial time series: A graph-theoretical approach*, Physics Letters A, 380(20), 1689 (2016); https://doi.org/10.1016/j.physleta.2016.03.011.
[42] B. Acosta-Tripailao, D. Pastén, P.S. Moya, *Applying the horizontal visibility graph method to study irreversibility of electromagnetic turbulence in non-thermal plasmas*, Entropy, 23(4), 470 (2021); https://doi.org/10.3390/e23040470.
[43] M. Zanin, D. Papo, *Algorithmic approaches for assessing irreversibility in time series: Review and comparison,* Entropy, 23(11), 1474 (2021); https://doi.org/10.3390/e23111474.

[44] A. Kiv, A. Bryukhanov, V. Soloviev, A. Bielinskyi, T. Kavetskyy, D. Dyachok, I. Donchev, V. Lukashin, *Complex network methods for plastic deformation dynamics in metals*, Dynamics, 3(1), 34 (2023); https://doi.org/10.3390/dynamics3010004.
[45] A.B. Kousaalya, B. Ayalew, S. Pilla, *Photopolymerization of acrylated epoxidized soybean oil: A photocalorimetry-based kinetic study*, ACS Omega, 4(26), 21799 (2019); https://doi.org/10.1021/acsomega.9b02680.
[46] M. Lebedevaite, J. Ostrauskaite, E. Skliutas, M. Malinauskas, *Photoinitiator free resins composed of plant-derived monomers for the optical μ-3D printing of thermosets*, Polymers, 11(1), 116 (2019); https://doi.org/10.3390/polym11010116.
[47] M. Bodor, A. Lasagabáster-Latorre, G. Arias-Ferreiro, M.S. Dopico-García, M.-J. Abad, *Improving the 3D printability and mechanical performance of biorenewable soybean oil-based photocurable resins*, Polymers, 16(7), 977 (2024); https://doi.org/10.3390/polym16070977.
[48] R. Saraswat, Shagun, A. Dhir, A., A.S.S. Balan, S. Powar, M. Doddamani, *Synthesis and application of sustainable vegetable oil-based polymers in 3D printing,* RSC Sustainability, 2(6), 1708 (2024); https://doi.org/10.1039/d4su00060a.
[49] Y. Zhang, H. Zhang, X. Zhao, *In-situ interferometric curing monitoring for digital light processing based vat photopolymerization additive manufacturing*, Additive Manufacturing, 81, 104001 (2024); https://doi.org/10.1016/j.addma.2024.104001.

Т.С. Кавецький[1,2,3], О.І. Мацьків[1], О. Шауша[2,4], Г. Швайдленкова[4,5], В.М. Соловйов[3,7], А.О. Бєлінський[6,7], А.В. Тужиков[3], Й. Остраускайте[8], А.Ю. Ків[3,9]

Кореляція між утворенням вільних радикалів та перетворенням подвійних зв'язків під час фотополімеризації за допомогою досліджень EPR і NIR та підходу теорії складних систем

[1]*Дрогобицький державний педагогічний університет імені Івана Франка, Дрогобич, Україна, kavetskyy@yahoo.com, omackiv@gmail.com;*
[2]*Інститут фізики Словацької академії наук, Братислава, Словаччина;*
[3]*Південноукраїнський національний педагогічний університет імені К.Д. Ушинського, Одеса, Україна, kiv.arnold20@gmail.com, vnsoloviev2016@gmail.com;*
[4]*Кафедра ядерної хімії, ФПН, Університет Коменського, Братислава, Словаччина, ondrej.sausa@savba.sk, helena.svajdlenkova@savba.sk;*
[5]*Інститут полімерів, Словацька академія наук, Братислава, Словаччина;*
[6]*Державний університет економіки і технологій, Кривий Ріг, Україна;*
[7]*Київський національний економічний університет імені Вадима Гетьмана, Київ, Україна;*
[8]*Каунаський технологічний університет, Каунас, Литва;*
[9]*Негевський університет Бен-Гуріона, Беер-Шева, Ізраїль*

Досліджено фотополімеризацію акрилованої епоксидованої соєвої олії (AESO) та ваніліндиметакрилату (VDM) з фотоініціатором (2,2-диметокси-2-фенілацетофеноном) (DMPA) in-situ за допомогою методів електронного парамагнітного резонансу (EPR) та ближньої інфрачервоної (NIR) спектроскопії. Виявлено кореляцію між концентрацією вільних радикалів, визначеною зі спектрів EPR, та площею піку перетворення подвійних зв'язків, визначеною зі спектрів NIR, як функцію часу УФ-опромінення для досліджуваного полімерного композиту. Спостережувана кореляція добре узгоджується з прогнозом явищ фотополімеризації та фотодеградації у межах підходу теорії складних систем.

Ключові слова: фотополімеризація, фотодеградація, ультрафіолетове світло, опромінення, полімери, композит, ЕПР спектроскопія, ІЧ спектроскопія, структура, властивості, теорія складних систем.